



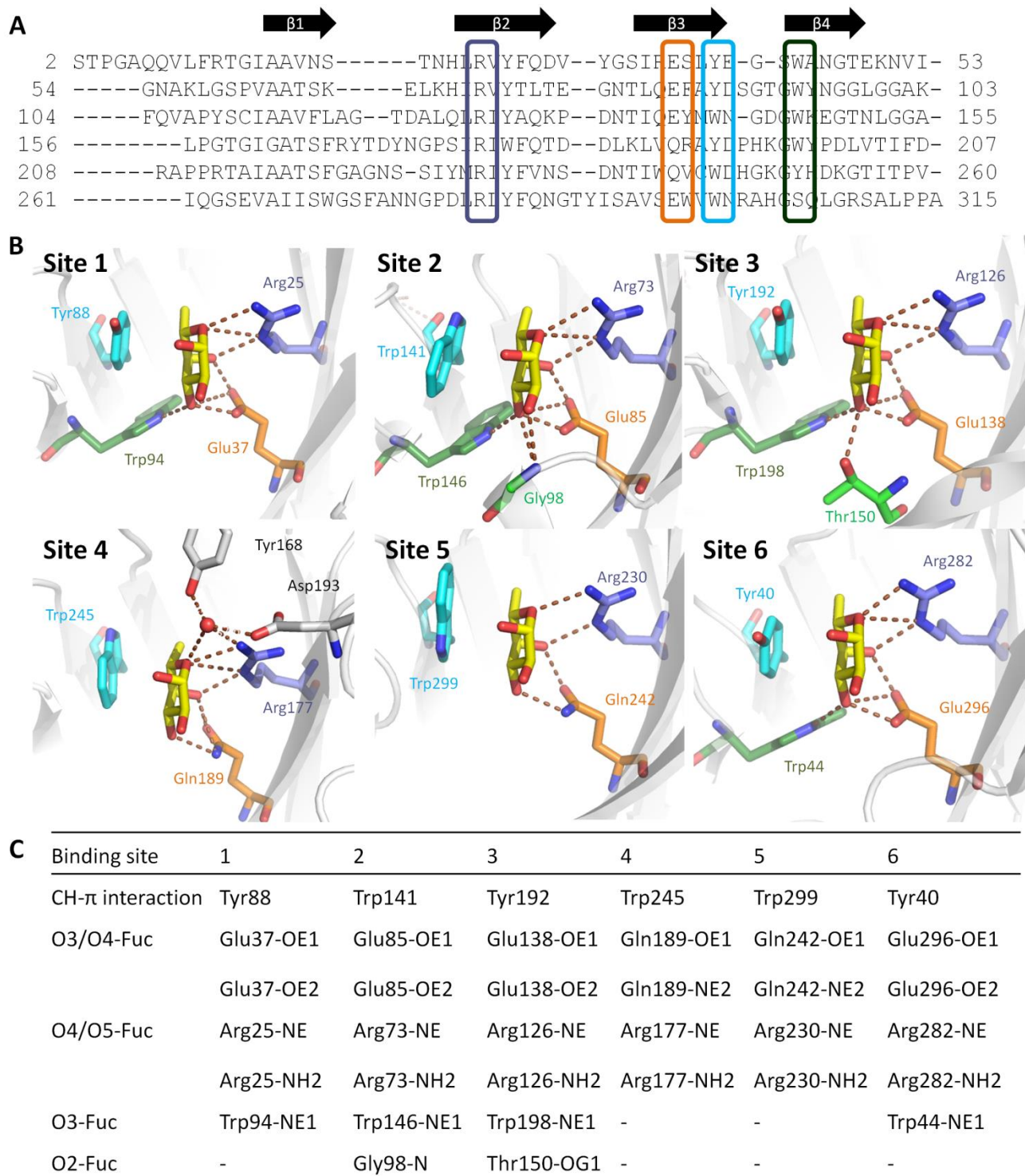
BIOLOGICAL  
CRYSTALLOGRAPHY

**Volume 71 (2015)**

**Supporting information for article:**

**Structural insights into *Aspergillus fumigatus* lectin specificity -  
AFL binding sites are functionally non-equivalent**

**Josef Houser, Jan Komarek, Gianluca Cioci, Annabelle Varrot, Anne Imberty  
and Michaela Wimmerova**



Modified from: Houser, J., Komarek, J., Kostlanova, N., Cioci, G., Varrot, A., Kerr, S. C., Lahmann, M., Balloy, V., Fahy, J. V., Chignard, M., Imberty, A. & Wimmerova, M. (2013). *Plos One* 8, doi: 10.1371/journal.pone.0083077.

**Figure S1** AFL binding sites. (A) The sequence of AFL six repetitions with indication of main secondary structure elements. Conserved amino acids directly involved in Fuc binding are highlighted by color box corresponding to panel B. (B) The six AFL binding sites of chain A of AFL/Fuca1-6GlcNAc complex. Fucosyl part of the Fuca1-6GlcNAc ligand shown in yellow. Colour code: cyan – stacking residue Tyr/Trp, dark blue – conserved Arg, orange – conserved Glu/Gln, dark green – H-bond-forming Trp, light green – other residues forming H-bonds to the Fuc. Water molecule involved in sugar binding in site 4 shown as red sphere, residues coordinating this water molecule shown in white. Hydrogen bonds participating in the ligand binding shown as brown dashed lines. The rest of the protein shown as a cartoon. (C) The overview of main fucose-binding amino acids in AFL complexes.

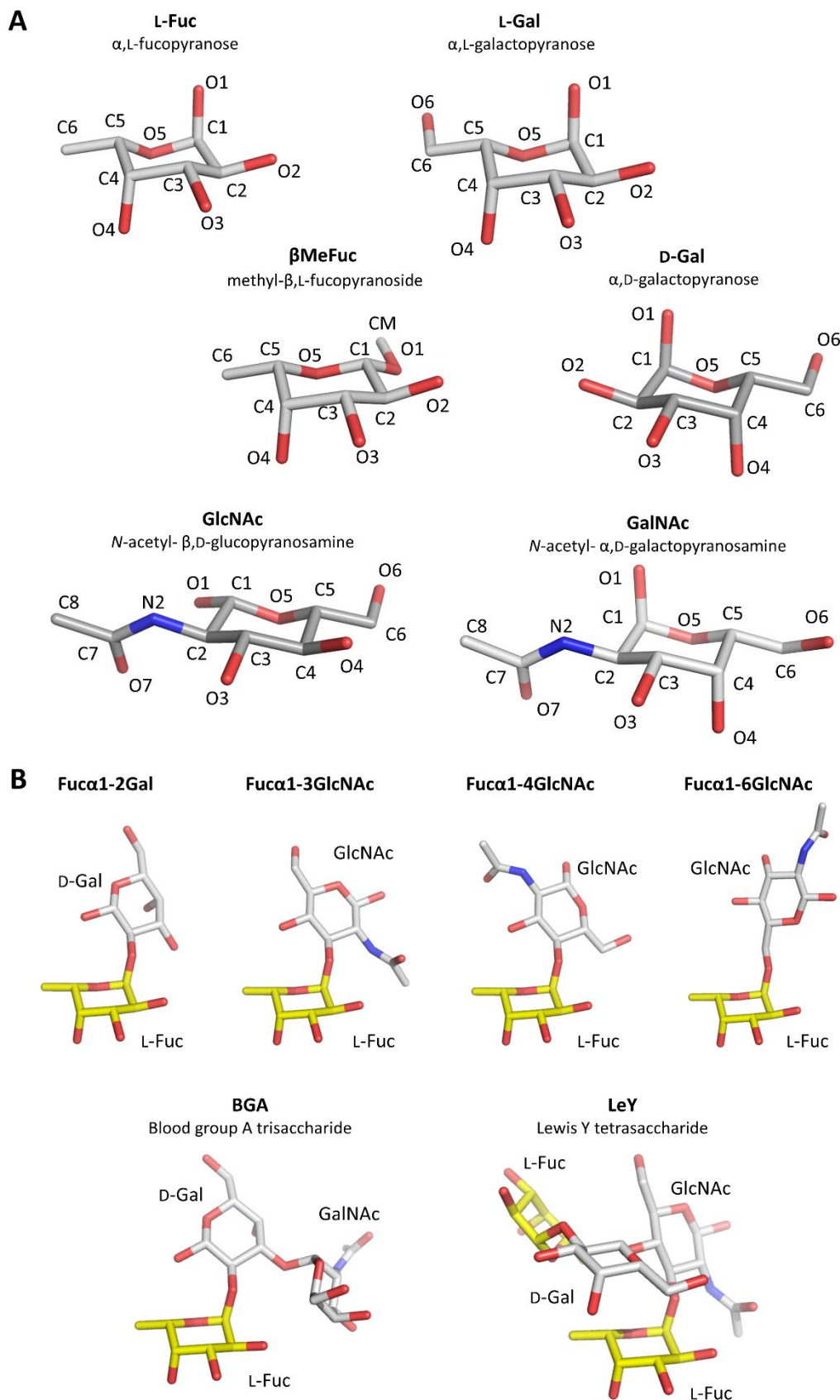


**Figure S2** Saccharides used in the structural study. (A) The monosaccharide units including the numbering of atoms. (B) The theoretical structures of di-, tri- and tetra- saccharides used for crystallization and structure analysis, based on Glycam - Carbohydrate builder (Woods group, 2005-2014). Fucosyl residues are shown in yellow, other saccharide units in white.

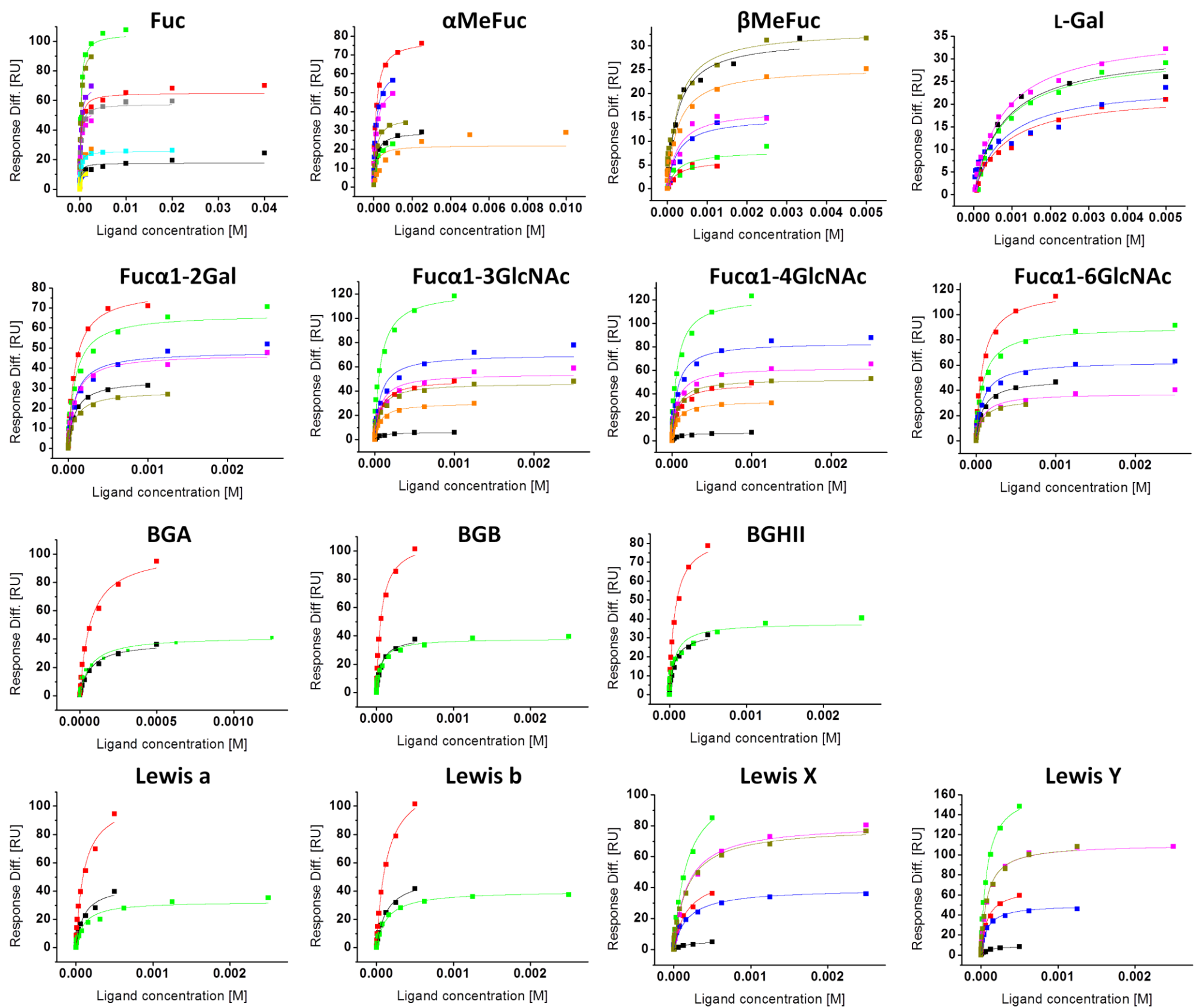


**Figure S3A** SPR steady-state measurement of interaction between AFL and various ligands. The ligands in increasing concentrations were injected onto AFL-modified chip surface. Relative responses at steady state were plotted against concentration and data fitted by one-site (Fig. S3A) or two-site (Fig. S3B) binding model, respectively. Individual measurements in each panel are distinguished by color.

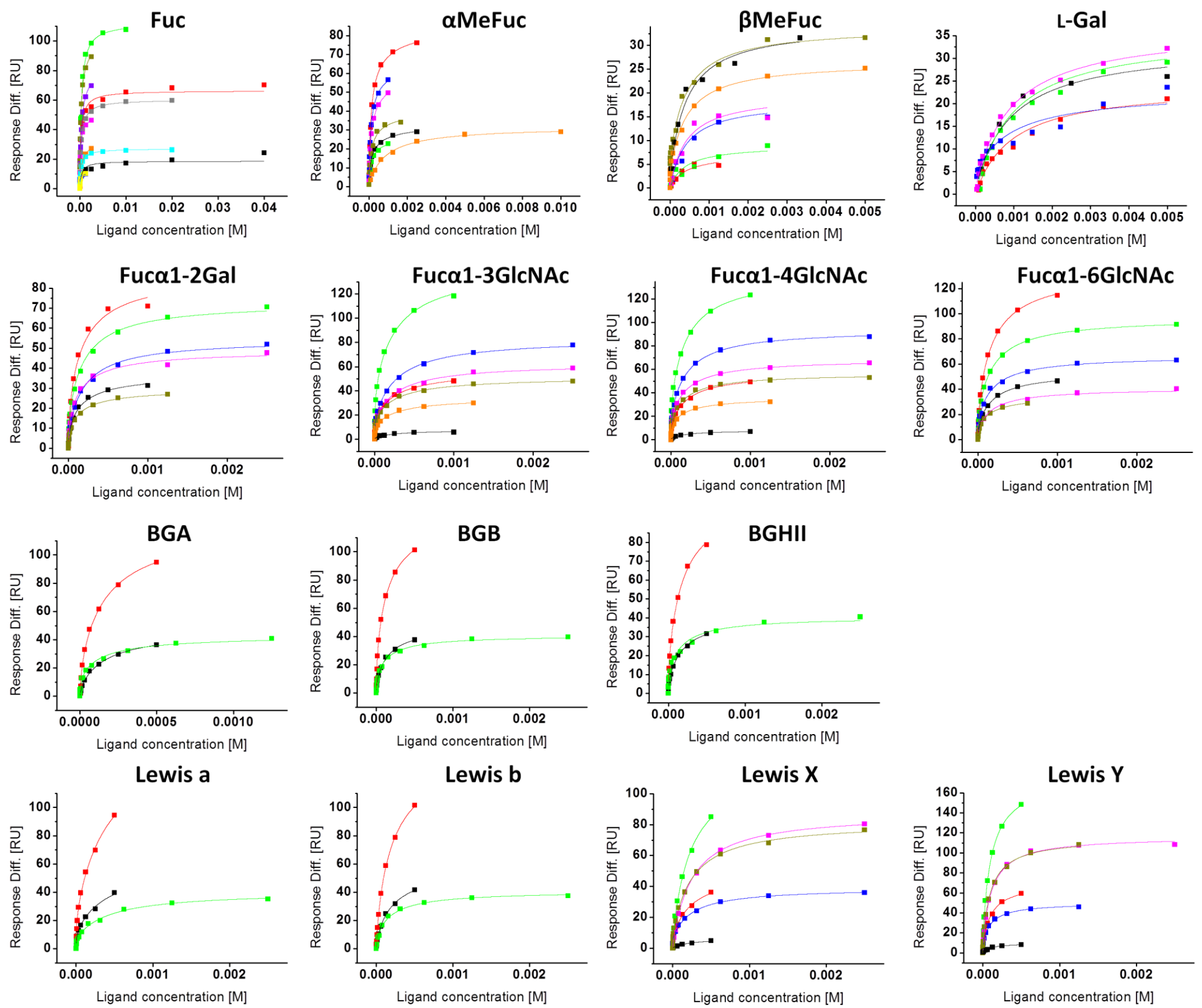


**Figure S3B** SPR steady-state measurement of interaction between AFL and various ligands. The ligands in increasing concentrations were injected onto AFL-modified chip surface. Relative responses at steady state were plotted against concentration and data fitted by one-site (Fig. S3A) or two-site (Fig. S3B) binding model, respectively. Individual measurements in each panel are distinguished by color.



<b>AAL</b>	1	---	PTRE	LYTSK	IAAIS	SWAAT	GGRQ	QRVY	FQ	LN	GKIRE	AQRGG	DNPW	TGGSS	QNVIG	EAKL	ESPL	AAV	66		
<b>AFL</b>	2	S	TPGA	QQVI	FR	GIAAVN	----	STNHL	RVYF	QIVY	GS	SIRE	SLYEG	S--	WANG	TEKN	VIGN	AKL	GSPVAA-	64	
<b>AAL</b>	67	TW	SAQGI	QIRV	YCVN	K	N	ILSE	FVYD	-GSK	WITG	QLGS	VGVK	VGS	N	SKLA	ALQW	GGSE	SAPP	NIRVYYQ	135
<b>AFL</b>	65	--	TSKEL	KHIR	VYTL	TEGNT	LQEF	AYDS	GTGW	YNGGL	GGAK	FQVA	PY	SCIA	AAV	LAGT	DAL--	QLRI	YAAQ	130	
<b>AAL</b>	136	KSN	LSGSS	IHEY	VWSG	K-W	TAGAS	FGST	APGT	GIGAT	AI-----	GPGR	LRIY	YQAT	DNK	IREH	CWDS	NS	198		
<b>AFL</b>	131	KPD	---	N	TIQE	YMWNG	DGWKE	CTNL	GGA	L	PCTG	IGAT	SFRY	TDYN	GPS-	IRIW	FQTD	DLKL	VQRAYD	PHK	196
<b>AAL</b>	199	-WY	--	VGGF	SASAS	AGVS	IAAIS	SWG	STPN	---	IRVY	WQK	GREEL	YEAY	--	GGSW	NTPG	QIKD	ASRPT	PS	260
<b>AFL</b>	197	GW	YDLV	TIFDR	AP	PTAIA	AATSE	FGAG	NSSI	YMRI	YVNS	DN	TIWQ	VCWD	HGKY	HDKG	TITPV	-----	260		
<b>AAL</b>	261	LP	DTFI	AANSS	----	GNID	ISVFF	QAS	SG--	VSLQ	QWQW	ISGK	GWSIG	-AVV	PTGT	PAGW	312				
<b>AFL</b>	261	IQ	GEVA	TIIS	WGSF	ANNGP	DLRL	YFQNG	TYIS	AVSE	WVWN	RAHGS	QLGR	SALPPA	-----	315					

**Figure S4** Sequence alignment of AAL and AFL proteins. Residues on the dimer interface are boxed, residues forming intermonomeric hydrogen bonds are marked with full (AFL) or empty (AAL) stars.

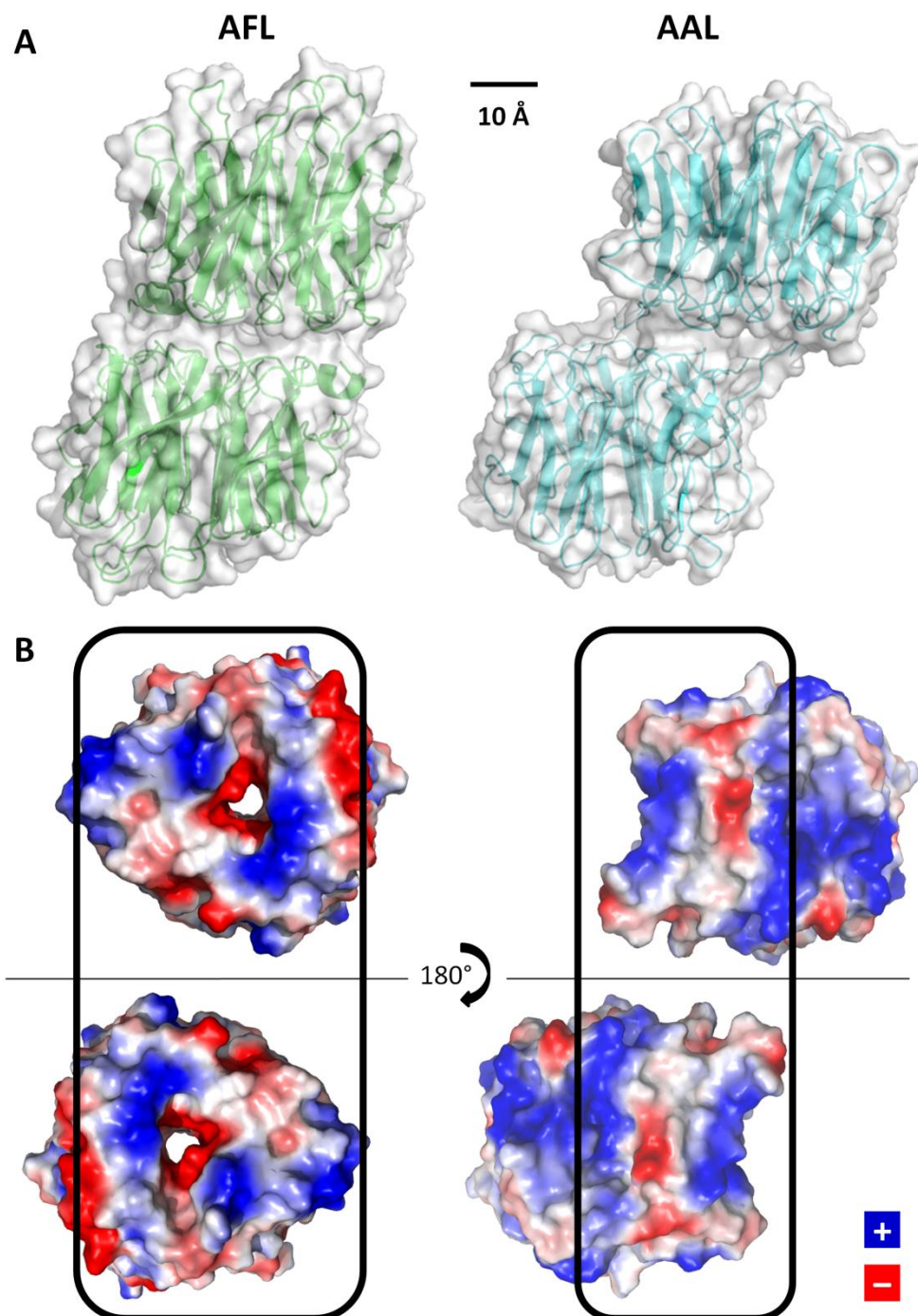


**Figure S5** Dimer formation of AFL and AAL. (A) Monomers are differently shifted with respect to each other in AFL and AAL dimer. (B) The contacting surface of both molecules in AFL and AAL dimers. The upper and lower molecule correspond to the upper and lower molecule in panel A. Differences in dimer formation are determined also by positive and negative side-chain organization (shown in blue and red, respectively). The interfacing parts of the monomer are framed.

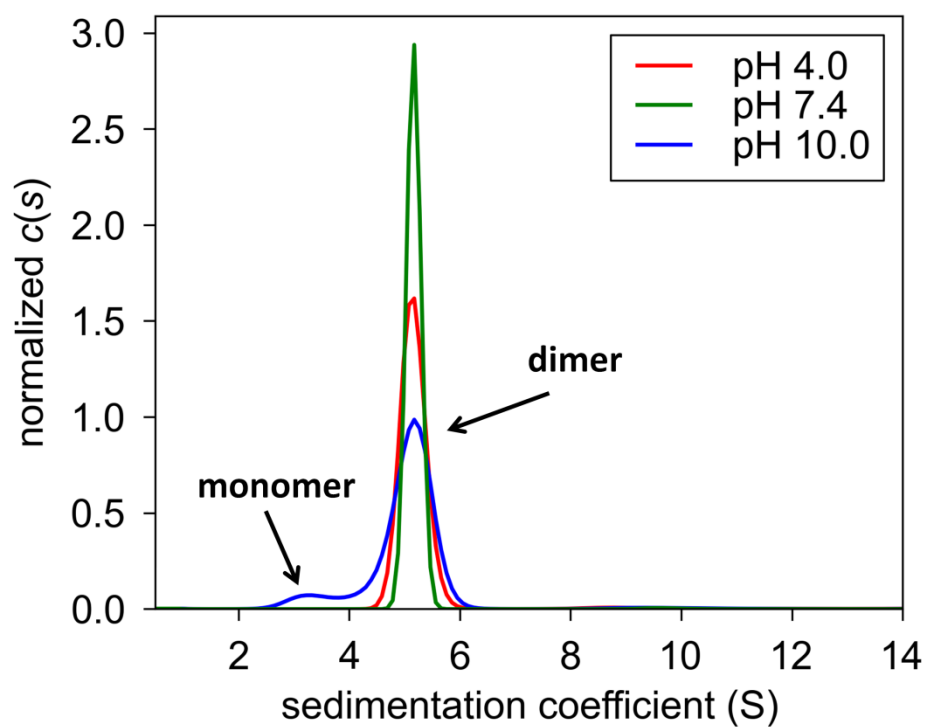


**Figure S6** AFL oligomeric state at various pH determined by AUC. Peaks are normalized to area. Dimer is stable at pH 4 (red line) and pH 7.4 (green line), at pH 10 (blue line), the peak of the monomer appears.



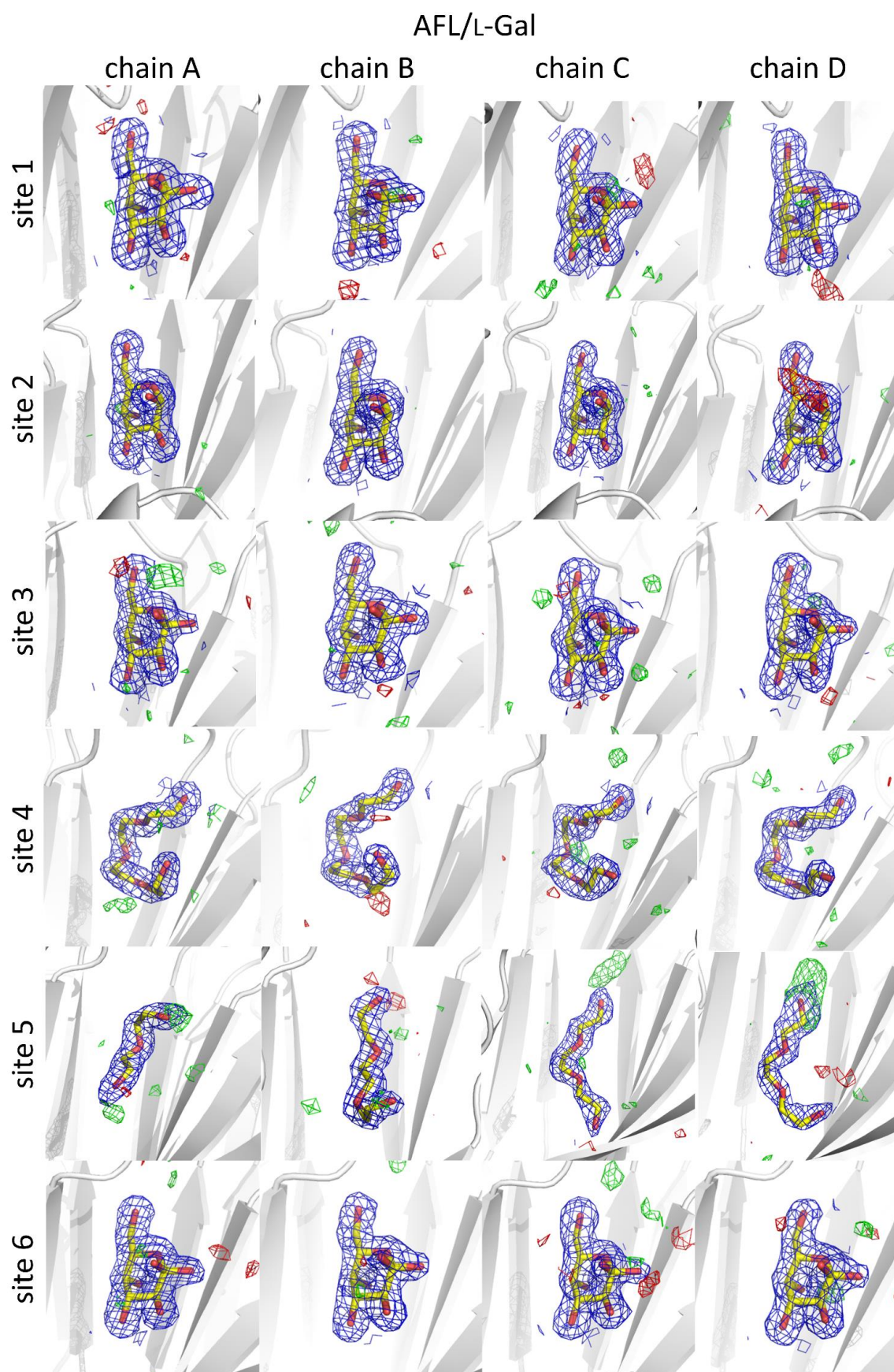


**Figure S7A** Binding sites of all AFL complexes analyzed. Assigned ligands are shown as sticks. In the sites with no ligand, the present water molecules are shown as spheres. Electron densities corresponding to ligands (2mFo-DFc map at  $\sigma = 1.0, 2.0$  Å cut off) shown in blue. Positive residual electron densities shown in green (mFo-DFc map at  $\sigma = 3.0, 4$  Å cut off) and negative in red (mFo-DFc map at  $\sigma = -3.0, 4$  Å cut off). (A) AFL/L-Gal, (B) AFL/ $\beta$ MeFuc, (C) AFL/Fuc $\alpha$ 1-6GlcNAc and AFL/fucosylated disaccharide mixture, (D) AFL/BGA and AFL/Le<sup>Y</sup>.

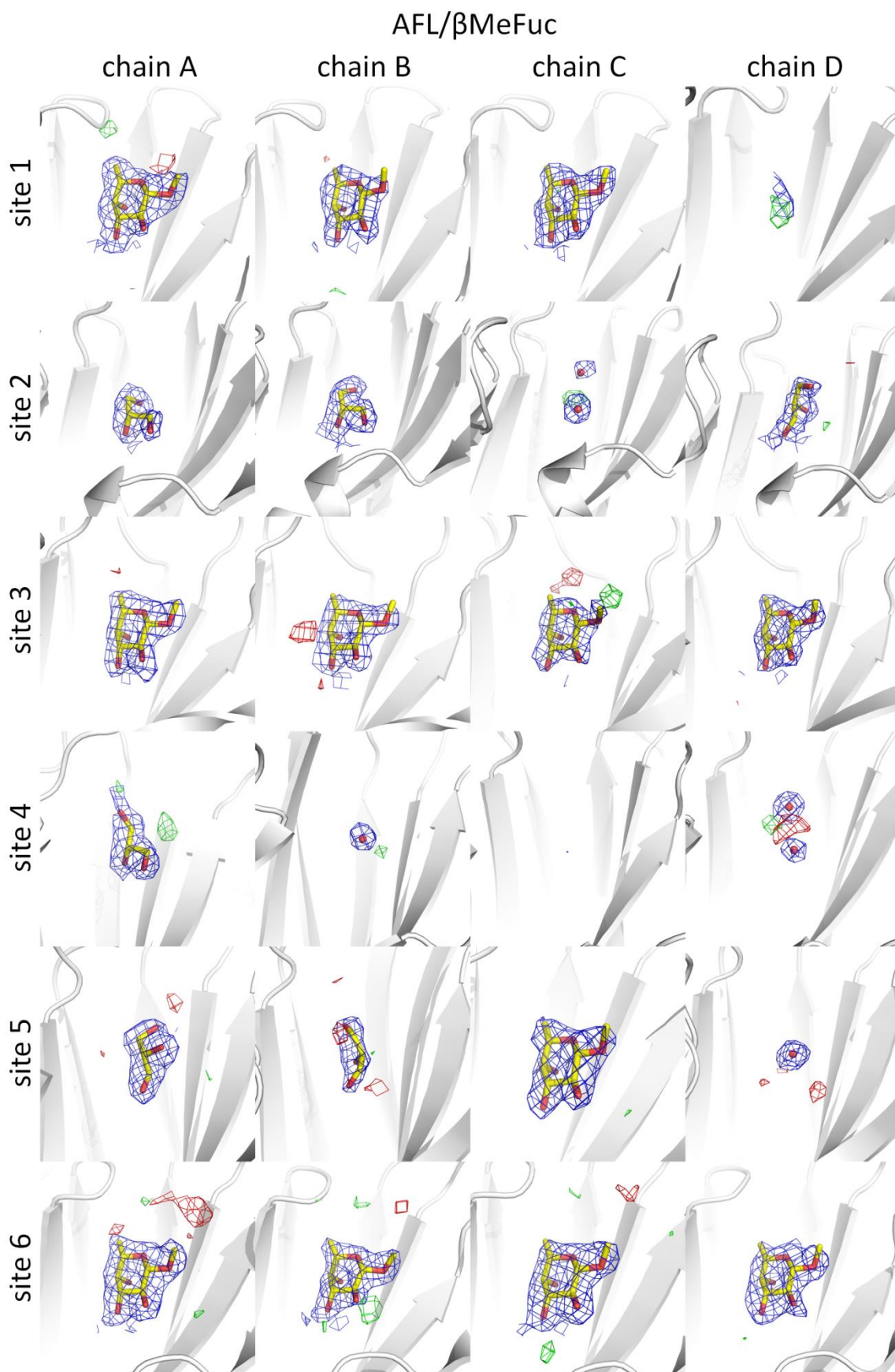


**Figure S7B** Binding sites of all AFL complexes analyzed. Assigned ligands are shown as sticks. In the sites with no ligand, the present water molecules are shown as spheres. Electron densities corresponding to ligands (2mFo-DFc map at  $\sigma = 1.0, 2.0$  Å cut off) shown in blue. Positive residual electron densities shown in green (mFo-DFc map at  $\sigma = 3.0, 4$  Å cut off) and negative in red (mFo-DFc map at  $\sigma = -3.0, 4$  Å cut off). (A) AFL/L-Gal, (B) AFL/ $\beta$ MeFuc, (C) AFL/Fuc $\alpha$ 1-6GlcNAc and AFL/fucosylated disaccharide mixture, (D) AFL/BGA and AFL/Le<sup>Y</sup>.



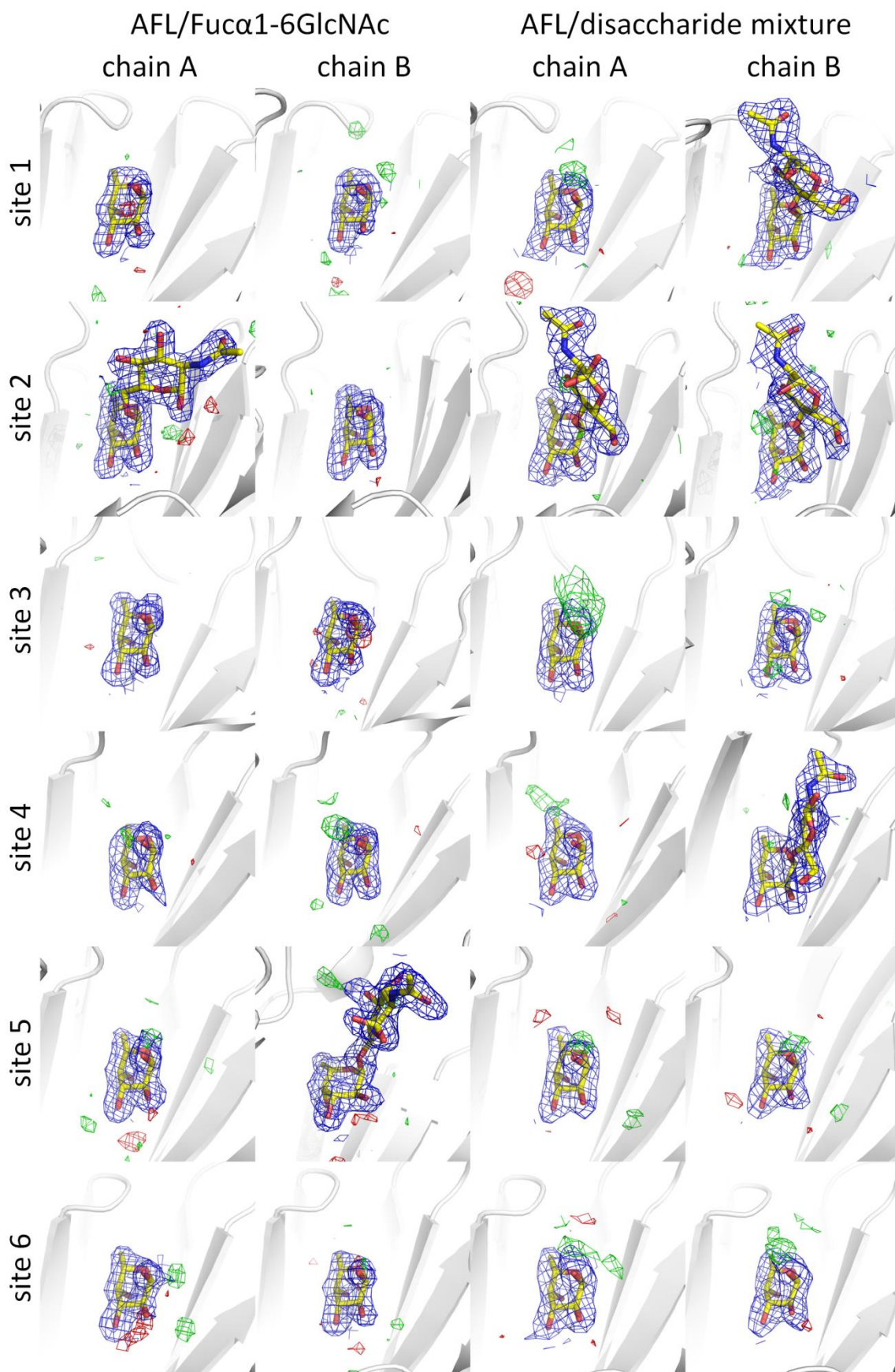


**Figure S7C** Binding sites of all AFL complexes analyzed. Assigned ligands are shown as sticks. In the sites with no ligand, the present water molecules are shown as spheres. Electron densities corresponding to ligands (2mFo-DFc map at  $\sigma = 1.0, 2.0$  Å cut off) shown in blue. Positive residual electron densities shown in green (mFo-DFc map at  $\sigma = 3.0, 4$  Å cut off) and negative in red (mFo-DFc map at  $\sigma = -3.0, 4$  Å cut off). (A) AFL/L-Gal, (B) AFL/ $\beta$ MeFuc, (C) AFL/Fuc $\alpha$ 1-6GlcNAc and AFL/fucosylated disaccharide mixture, (D) AFL/BGA and AFL/Le<sup>Y</sup>.

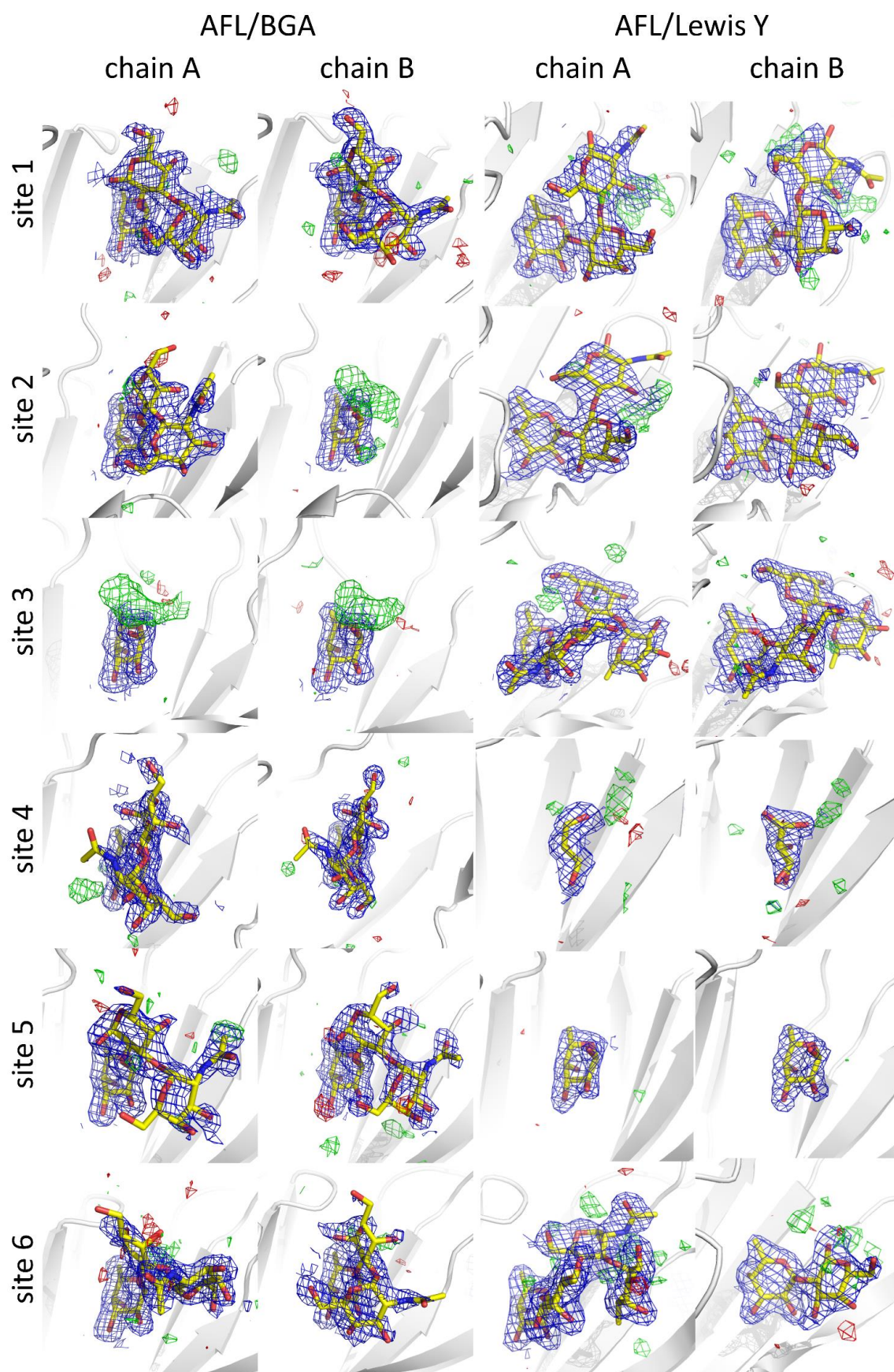


**Figure S7D** Binding sites of all AFL complexes analyzed. Assigned ligands are shown as sticks. In the sites with no ligand, the present water molecules are shown as spheres. Electron densities corresponding to ligands (2mFo-DFc map at  $\sigma = 1.0, 2.0$  Å cut off) shown in blue. Positive residual electron densities shown in green (mFo-DFc map at  $\sigma = 3.0, 4$  Å cut off) and negative in red (mFo-DFc map at  $\sigma = -3.0, 4$  Å cut off). (A) AFL/L-Gal, (B) AFL/ $\beta$ MeFuc, (C) AFL/Fuc $\alpha$ 1-6GlcNAc and AFL/fucosylated disaccharide mixture, (D) AFL/BGA and AFL/Le<sup>Y</sup>.



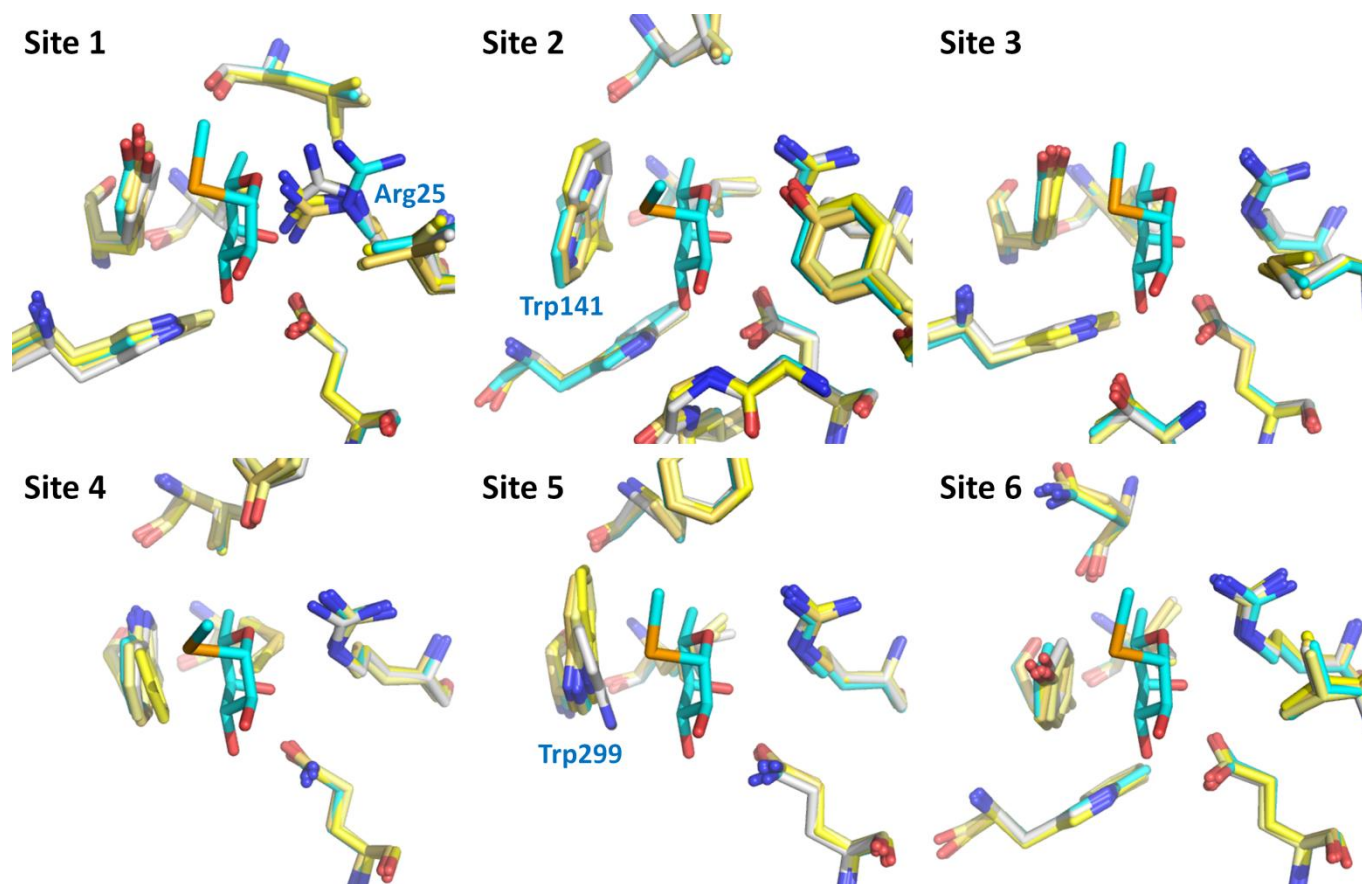


**Figure S8** Comparison of AFL binding sites without any ligand with the AFL/MeSeFuc complex. Only residues within 4 Å distance from MeSeFuc are shown. Four chains of free AFL are colored from white to yellow, AFL/MeSeFuc chain A is shown in cyan. Side chains with major position change are labeled.